Microporous and Mesoporous Materials 265 (2018) 227–233

Contents lists available at ScienceDirect

Microporous and Mesoporous Materials

journal homepage: www.elsevier.com/locate/micromeso

Carbon monoxide adsorption in ZIF-8: Kinetics and equilibrium

Dinuka H. Gallaba[a], Jhonny Villarroel-Rocha[b], Karim Sapag[b], Aldo D. Migone[a,*]

[a] Department of Physics, Southern Illinois University, Carbondale, IL 62901, USA
[b] Instituto de Fisica Aplicada, CONICET-Universidad Nacional de San Luis, San Luis, Argentina

ARTICLE INFO

Keywords:
Adsorption
Gate opening
Carbon monoxide
ZIF-8 2010 MSC: 00-01
99-00

ABSTRACT

We present the results of a study of the kinetics and equilibrium characteristics of CO sorption in ZIF-8. We measured adsorption isotherms at five temperatures between 72.67 and 104.58 K; all the isotherms exhibit three sub-steps below saturation. We have studied the evolution of the adsorption kinetics of this system by monitoring the equilibration times as a function of sorbent loading. We find that there is a very large, sharp maximum, in the equilibration times in the region corresponding to the highest loading sub-step in the sorption data; and we find a much smaller local maximum for loadings corresponding to the intermediate-loading sub-step. We have determined the isosteric heat of adsorption for CO in ZIF-8 and its dependence on sorbent-loading. We find a sharp isosteric heat of adsorption peak at values of the sorbent-loading corresponding to the highest loading isotherm sub-step. We discuss a possible explanation for the combined results of kinetic and isosteric results for this system. We have also studied the temperature evolution of the characteristics of the sub-steps present in the isotherms. We find that, as was the case for other systems in ZIF-8, the relative pressures at which the two higher-loading isotherm sub-steps occur move increasingly closer to the saturated vapor pressure as the isotherm temperatures increase.

1. Introduction

Over the past decade there has been an explosive growth in the study of gas sorption in porous metal-organic framework (MOF) materials [1–5]. Porous MOFs are constituted by metallic ions connected to organic linkers, forming a material in which there are crystallographically determined arrays of pores forming part of the material's structure [6,7]. If the linkers and/or the metallic ions used in the synthesis of a porous MOF are changed, the resulting pore structure will be altered (i.e., the pore size, volume, and in some cases the pore connectivity, will be changed) [1,6,7].

Porous MOFs offer a greater degree of controllability over the pore structure than that which is available in other classes of porous sorbents. This makes MOFs attractive candidates for practical use because, potentially, a porous MOF can be synthesized with a pore structure designed to meet a specific application [8].

Among the different classes of MOFs, there is a group that has structures similar to those of zeolites. These MOFs are called zeolitic imidazolate frameworks, or ZIFs [8–11]. ZIFs are considerably more stable thermally and chemically than other types of MOFs, making them appealing candidates for practical applications [8,10]. ZIF-8 is the most studied member of this group. ZIF-8 has a structure similar to that of sodalite, in which relatively large pores are interconnected through smaller diameter windows. [12].

One of the more intriguing features of gas sorption in ZIF- 8 is that adsorption isotherms measured at cryogenic temperatures for several, but not for all, gases in this sorbent exhibit sub-steps below saturation (either two or three sub-steps, depending on the sorbate) [10,12,13].

There have been different explanations proposed for the origin of the sorption sub-steps. The nature of the sub-steps remains a subject of some controversy. The first explanation for the sub-steps in N_2 and Ar sorption isotherms in ZIF-8, given by Park et al. (in the supplementary materials of the cited reference), was that they corresponded to a reorganization of the adsorbed gas molecules at a threshold pressure in an essentially inert ZIF-8 [10]. X-ray diffraction measurements conducted at room temperature and high-pressures, using a methanol-ethanol mixture as the pressure-transmitting fluid, reported a single-crystal to single-crystal transition in ZIF-8 at 1.47 GP [14]. The transition occurred as a result of the pressure-transmitting fluid being forced into the ZIF-8. The imidazolate linkers in the ZIF-8 reoriented themselves, increasing the size of the windows present in ZIF-8, and, there was an expansion in the volume of the ZIF-8 produced by the admission of the fluid into the ZIF-8 [14]. The ZIF-8 retained the same space-group symmetry that it had at ambient conditions [14]. Fairen-Jimenez et al., in a combined adsorption isotherm, X-ray diffraction, and computer simulation study for N_2 in ZIF-8, found that the same type of structural

* Corresponding author.
E-mail address: aldo@physics.siu.edu (A.D. Migone).

https://doi.org/10.1016/j.micromeso.2018.02.020
Received 7 November 2017; Received in revised form 29 January 2018; Accepted 17 February 2018
Available online 02 March 2018
1387-1811/

transition that was observed at high pressures also occurred as a result of the low-pressure sorption of N_2 at 77 K [12]. After the transition, the ZIF-8 experienced a slight volume expansion, maintained the same space-group symmetry, and, exhibited a re-orientation of the imidazolate linkers (the sub-step in the isotherm was associated with the sorption-induced structural phase transition) [12]. The phenomenon of linker re-orientation in the structural transition is referred to as "gate-opening". Ania et al. conducted a detailed adsorption isotherm and GCMC simulation study for N_2, CO, Ar and O_2 at 77 K and at 90 K [13]. This study reported for the first time the existence of three sub-steps below saturation for both N_2 and CO in ZIF-8, at both temperatures. By contrast, only two sub-steps were present for Ar and O_2 in ZIF-8 [13]. The highest-loading sub-step for all four gases was interpreted as corresponding to the expansion of the ZIF-8 framework upon adsorption [13]. For N_2 and CO the highest loading sub-step was explained as a rearrangement of the sorbed molecules resulting from electrostatic interactions between the ZIF-8 and these two polar sorbates [13]. The intermediate-loading step for N_2 and CO was interpreted as signaling a gas-induced opening of the ZIF-8 structure (which would, presumably, involve gate-opening) [13]. Magdysuk et al. conducted an adsorption isotherm and synchrotron X-ray powder diffraction study of Xe in ZIF-8 [15]. X-ray data were collected as a function of loading, allowing the study of how the filling of the ZIF-8 sorption sites proceeds as loading increases. They observed gate-opening for this system [15]. Low-temperature adsorption isotherms for Xe in ZIF-8 were conducted between 95.00 and 157.56 K; this study reported the presence of a sub-step in the sorption data which was interpreted as gate-opening [16]. Casco et al. used 77 K adsorption isotherms and *in situ* inelastic neutron scattering to explore N_2 in ZIF-8. Comparing the scattering spectrum for bare ZIF-8 with that for a fully N_2-loaded ZIF-8 they were able to unequivocally determine that there was gate-opening for this system [17]. (The flipping of the imidazolate linkers gives rise to a distinctive inelastic neutron scattering signature, which is readily resolvable from signature for the bare ZIF-8) [17]. The same group has very recently conducted a combined inelastic neutron scattering and adsorption isotherm study (at 77 K) of the sorption of N_2, CO, Ar and O_2 in ZIF-8 [18]. This study found the signature for linker-flipping for N_2 and for CO, but not for O_2 or Ar. This group concluded that linker-flipping and structural deformation were responsible for the flexibility of ZIF-8 in the sorption of N_2 and CO; and that, since there was no evidence of flipping for O_2 nor Ar, only structural deformation was responsible for the flexibility of ZIF-8 in Ar and $O_{2\ \text{sorption.}}$ [18].

Significant structural response to gas sorption (whether it be gate-opening, or structural deformation) is unusual among sorbents. Many sorbents do not undergo structural phase transitions as a result of sorption processes, and can (for all practical purposes) be considered to be inert during sorption processes.

We present here the results of a study of the sorbent loading dependence of the kinetic and equilibrium sorption characteristics of CO in ZIF-8. After presenting the isotherms, we will discuss the results obtained for the adsorption kinetics (as it is determined from measuring the equilibration times) as a function of sorbent loading, the results for the dependence of the isosteric heat of adsorption on sorbent loading, and, the temperature evolution of the adsorption sub-steps.

2. Experimental

Most of the adsorption measurements conducted in this study were performed in an especially built setup. The pressures were measured using three capacitance manometers (of maximum ranges 10, 1000 and 25000 Torr), manufactured by MKS. The ZIF-8 sample used in these measurements had a mass of 0.1858 g; it was produced by BASF and sold by Sigma-Aldrich as Basolite Z1200. The sample was placed in the stainless steel cell in which the measurements were performed. The cell was sealed with a copper gasket and connected to a vacuum pumping station. Before starting the adsorption measurements, the sample cell was heated to 120 °C under a vacuum of $\sim 10^{-6}$ Torr for 12 h in order to activate the ZIF-8. The sorbent was not re-exposed to air after the activation process was concluded.

The sample cell is mechanically attached to a closed-cycle helium refrigerator, the operation of which enables the cell to reach the cryogenic temperatures at which the measurements were conducted. The temperature of the cell was controlled to within ± 25 mK using a two-stage temperature control arrangement. The Pt sensor used to determine the cells temperature was cross-calibrated against the carbon monoxide saturated vapor pressure: the saturated vapor pressures were measured in the isotherms, and these values were used to determine the cell temperature using NIST tables for the saturated vapor pressure of carbon monoxide [19]. The gas used in the measurements was Research Grade carbon monoxide from Matheson™. Data acquisition for the isotherms was carried out using an in-house developed program in LabView™ [16,20,21]. After the desired amount of gas was loaded into the dosing manifold, the valve isolating the sample cell from the rest of the dosing manifold was opened. The pressure was then measured as a function of time; the values for sorbent loading were obtained from the pressures. The valve between the cell and the dosing manifold remains open until just before the next dose of gas is added to the dosing manifold. Our setup allows us to monitor the kinetics of adsorption, i.e., how sorbent loading approaches equilibrium as a function of the time elapsed after gas is added to the cell. In order to account for the fact that the experimental cell is at a different temperature than the pressure gauges, we applied standard thermomolecular corrections [22] to the measured pressures (these corrections are only significant for pressures below 1 Torr). We have also conducted an adsorption-desorption isotherm for CO in ZIF- 8 at liquid nitrogen temperature. These measurements were conducted on a Micromeritics™ ASAP 2000 apparatus, equipped with 1, 10 and 1000 Torr transducers. The sample was previously degassed in vacuum at 120 °C for 12 h. The purpose of these measurements was to provide a direct comparison with the results for the CO in ZIF-8 system that are available in the literature [13,18]. The sample of ZIF-8 used in these adsorption-desorption measurements was selected from the same batch of commercial ZIF-8 from which the sample that was used for all of the other adsorption measurements.

3. Results

3.1. Isotherms

An adsorption-desorption isotherm was performed with the ZIF-8 in a glass bulb submerged in a liquid nitrogen bath. The measurements were performed and recorded using software provided by Micromeritics. These data are shown in Fig. 1. The data exhibit three sub-steps below saturation; there is a hysteresis loop present for the highest loading sub-step (the adsorption branch corresponds to the lower loading for a given pressure, while the desorption branch to the highest-loading). These data should be compared with that shown in Fig. 3 of reference [13]; the agreement between them is very good.

We measured adsorption isotherms at five temperatures: 72.67, 78.28, 85.30, 95.69, and 104.56 K. These data are presented in Fig. 2. The four lower temperature isotherms were continued until the saturated vapor pressure was reached.

Each of the four lower temperature isotherms displays four quasi-vertical sub-steps. The sub-step at the highest loadings and pressures corresponds to the CO reaching the saturated vapor pressure at the isotherm temperature. For the temperature range studied, saturation corresponds to liquid-vapor coexistence at equilibrium [19]. The three sub-steps present below saturation are similar to the ones that were previously reported for this system at 77 K [13,18] and at 90 K. [13].

The lowest-pressure sub-step encompasses the largest loading interval of the three present below saturation. The highest value of the loading for this low pressure sub-step increases with increasing temperature, going from just below 9400 μmol/g at 72.67 K, to

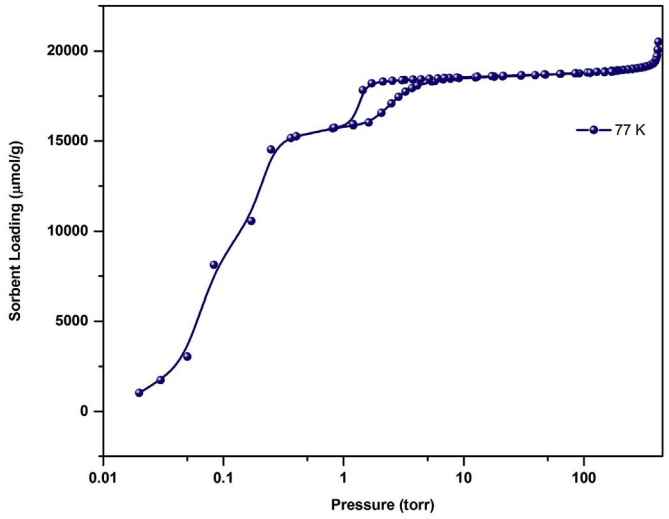

Fig. 1. Adsorption-desorption isotherm for CO in ZIF-8 at liquid nitrogen temperature. These data were measured in a Micromeritics ASAP 2000 apparatus.

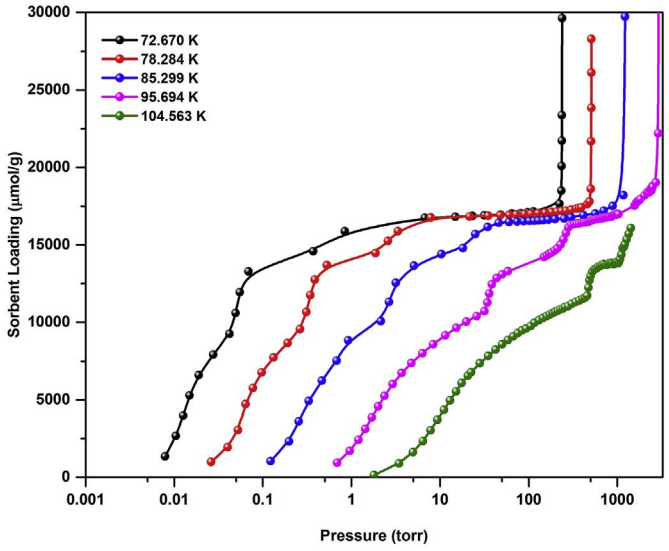

Fig. 2. Adsorption isotherms measured at 72.67, 78.28, 85.30, 95.89 and 104. 56 K. The large vertical step at the highest loadings (present for all except the highest temperature isotherm) corresponds to carbon monoxide reaching its saturated vapor pressure for the respective temperature.

10700 μmol/g at 95.69 K and 11700 μmol/g at 104.56K.

The intermediate loading sub-step is present between 9470 and 14260 μmol/g. The loading span corresponding to this sub-step becomes smaller as the isotherm temperature increases, decreasing by nearly a factor of two over the range of temperatures studied. This sub-step has been attributed to a structural transition (gate-opening) occurring in this system. [13,18].

The highest-loading sub-step below saturation spans the smallest loading interval: it is covers, roughly, a 1880 μmol/g loading interval. This sub-step, as noted in the introduction, was attributed to a reorganization of the sorbed molecules after sorbent expansion.

3.2. Kinetics of adsorption

We have measured the time interval needed for equilibrium to be reached after gas is added to the cell containing the ZIF-8 along the isotherms. We monitor how the amount of CO sorbed increases as a function of time as equilibrium is approached [16,20,21]. During the approach to equilibrium the amount of gas in the sorbent is determined

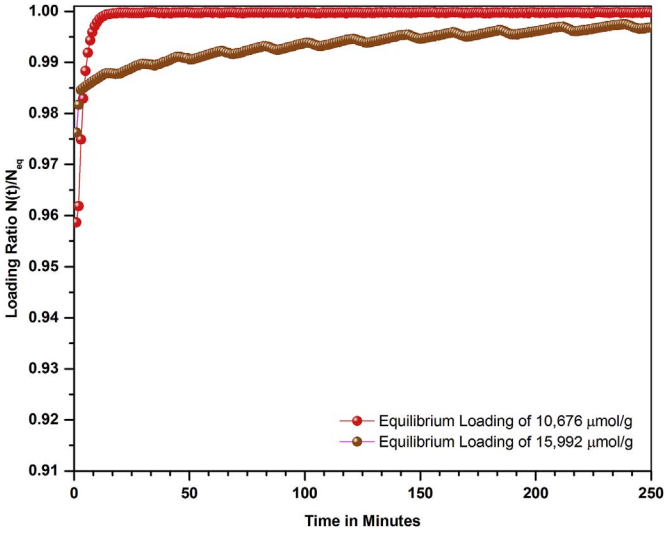

Fig. 3. Time dependence of the fractional loading increase of the ZIF-8 after a dose of gas is added to the sample cell for the CO isotherm at 95.69 K. The curves correspond to equilibrium sorbent loadings in the highest-loading sub-step region (15,992 μmol/g, bottom curve) and at a loading well below it (10,676 μmol/g, top curve). When the loading reaches its equilibrium value, the curves become parallel to the horizontal axis. It is clear that the equilibration time is much longer for highest-loading sub-step region (note that in the data presented in this graph, equilibrium has not yet been reached in the highest-loading substep region after more than 4 h have elapsed).

following the same procedure used to determine the loading once equilibrium is established; i.e., subtracting the amount of CO that is present in the vapor phase in the cell at a given time, from the total amount of gas dosed into the cell. (We have accounted for the pressure drop that results from gas expansion into the cell when the gas is admitted into the cell in these calculations.) During equilibration, the amount of CO present in the cell in the vapor phase decreases as a function of time. The time required for equilibrium loading to be reached after a dose of gas is added is the equilibration time.

Data corresponding to the time evolution of the fractional loading [i.e., $n(t)/n_{eq}$, with n(t) the sorbent loading at time t after the gas was dosed into the cell, and, n_{eq} the equilibrium value of the loading for that dose] are presented in Fig. 3 for two equilibrium loading values (15992 μmol/g, and at 10676 μmol/g). The two curves have been displaced along the vertical axis for the sake of clarity.

In Fig. 4 we present a summary of results for the equilibration times as a function of loading for the 95.69 K isotherm. The times shown in the y axis of Fig. 4 are those at which sorbent loading reaches 99.9% of the respective equilibrium value [23]. The reason for choosing the time required to reach 99.9% of equilibrium loading rather than the time required to reach equilibrium in Fig. 4 is that this choice reduces the noise in the data, thus, allowing for an easier identification of the trends exhibited by the equilibration times [24]. In every case we have extended the measurements until well after equilibrium was reached for each loading; this was done to ensure that there was no ambiguity regarding what the values for the equilibrium loading and equilibrium pressure are.

While equilibration times are generally decreasing with increasing loading up to approximately 11000 μmol/g; at loadings above that there are two noticeable exceptions to the decreasing trend. There is a maximum in the equilibration time near 13000 μmol/g, and, there is a much larger and sharper maximum in equilibration times near 16000 μmol/g. Beyond 16000 μmol/g, the equilibration times drop precipitously.

Comparing with the isotherm data in Fig. 2 we note that the two regions where the equilibration times increase correspond, respectively, to the loadings at which the intermediate-loading sub-step and the highest loading sub-step occur in the isotherms. An increase in the time

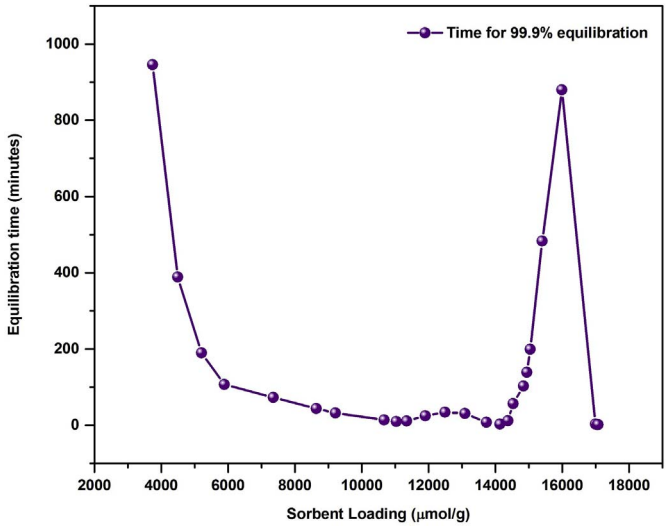

Fig. 4. The time needed to reach 99.9% of the equilibrium loading value after a dose of gas is added to the cell containing the ZIF-8 is plotted as a function of the equilibrium loading value, for the 95.69 K isotherm There are two maxima in the data: a small maximum near a loading of 13,000 μmol/g and a very large and sharp maximum at a loading near 16,000 μmol/g. These peaks are centered, respectively, at the midpoints of the segments of the isotherm corresponding to the intermediate loading sub-step, and, to the higher-loading sub-step.

required to reach equilibrium at the highest-loading sub-steps for CO and for N_2 in ZIF-8 was noted in ref. [13]. The maximum in equilibration times being reported here for loadings corresponding to the intermediate-loading sub-step had not been previously observed.

3.3. Evolution of isotherm features with temperature

The values of the relative pressures (i.e., p/p_o, where p_o is the saturated vapor pressure corresponding to the isotherm temperature; and p the pressure at the midpoint of the sub-step) at which the intermediate-loading sub-step and the highest-loading sub-step occur change significantly as a function of temperature. The relative pressures for both sub-steps approach $p/p_o = 1$ as the temperature increases. That this is indeed the case is most readily seen by plotting the logarithm of the pressure at the mid-point of the sub-steps as a function of the inverse of the isotherm temperature (Fig. 5). Also shown in Fig. 5 is the logarithm of the saturated vapor pressure for CO as a function of the inverse of the temperature. As is apparent in Fig. 5, the straight lines obtained for the intermediate- and highest-loading sub-steps will eventually intersect the line corresponding to the saturated vapor pressure.

3.4. Isosteric heat of adsorption

We have obtained the isosteric heat of adsorption, $(q_{st})_n$, at a given value, n, of the loading for CO in ZIF-8 from the isotherm data by using (1) [25].

$$(q_{st})_n = k_B T^2 \left(\frac{\partial Log(p)}{\partial T}\right)_n \quad (1)$$

This equation is analogous to the Clausius-Clapeyron equation, with $(q_{st})_n$, the isosteric heat of adsorption for a fixed n, taking the place of the latent heat of transition. When this differential equation is solved assuming ideal gas behavior for the vapor the following result is obtained:

$$Log(p) = -\frac{(q_{st})_n}{k_B T} + b \quad (2)$$

In practice, to obtain $(q_{st})_n$ what is done is to plot the Log(p) for that fixed amount of sorbent loading, n, as a function of the inverse of the isotherm temperature. It is clear from (2) that the slope of the straight line that results from this plot is directly proportional to $(q_{st})_n$, the isosteric heat of adsorption for the loading, n, of the sorbent. When this process is repeated for a number of different loadings, we obtain the loading dependence of the isosteric heat of adsorption. The result for the loading dependence of $(q_{st})_n$ is presented in Fig. 6.

There are two peaks in the isosteric heats dependence on loading. The broad peak is centered near the mid-point of the intermediate-loading sub-step, and, the much sharper peak that occurs at a loading corresponding to the highest-loading sub-step in the isotherms.

For loadings measured at the saturated vapor pressure the value obtained for the isosteric heat by this process should agree with the heat of vaporization for CO (for the temperatures and pressures at which these isotherms were measured saturation corresponds to liquid-vapor coexistence). This is the case: the average isosteric heat determined for loadings at the saturated vapor pressure is 61.9 meV/molecule (or 5.9 kJ/mol), in excellent agreement with the value of 62.4 meV/molecule (or 6.0 kJ/mol) reported for the latent heat of vaporization for CO for the interval between 68 K and 108 K [26]. The fact that the bulk value is reproduced provides an internal consistency check for the isosteric heat of adsorption values that we have determined here.

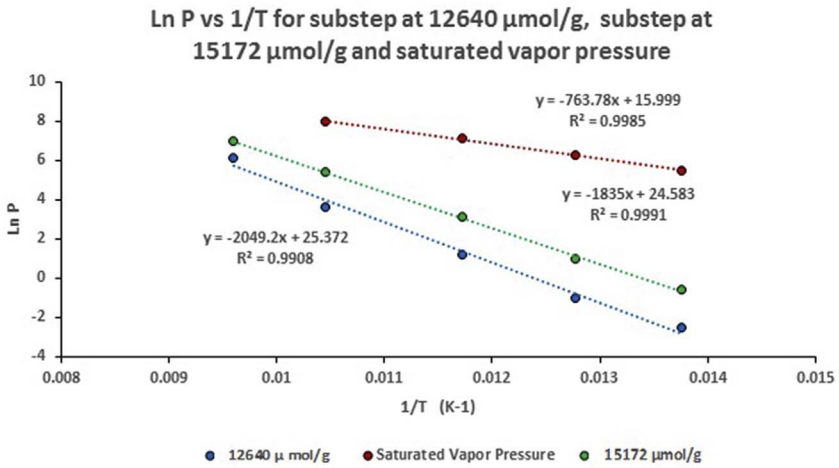

Fig. 5. Straight lines that result from plotting the logarithm of the saturated vapor pressure (top line), the logarithm of the pressure at the midpoint of the higher loading sub-step, and the logarithm of the pressure at the midpoint of the intermediate loading sub-step (bottom line), as a function of the inverse of the isotherm temperature.

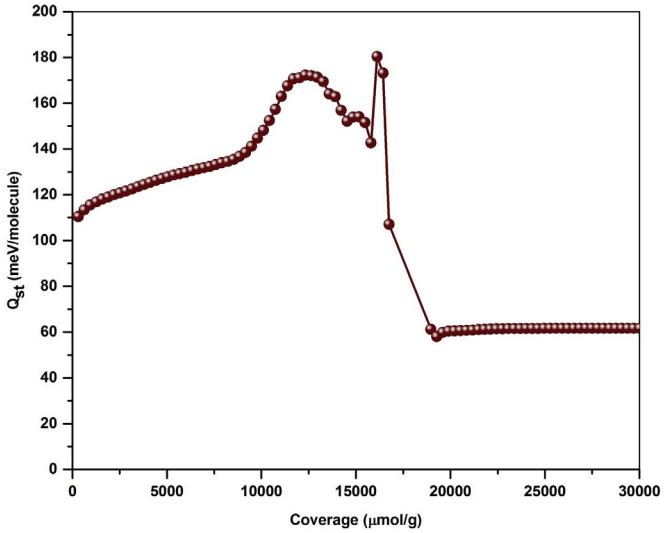

Fig. 6. Isosteric heat of adsorption as a function of sorbent loading. There is a broad peak near 12500 μmol/g and a sharp peak at 16500 μmol/g. These loadings correspond, respectively, to the midpoints of the intermediate loading sub-step, and to the higher loading sub-step. The constant value of the isosteric heat of adsorption at the highest loadings shown (i.e. at saturation) corresponds to the bulk latent heat of vaporization for CO.

4. Discussion

4.1. Kinetics

The behavior of the sorption kinetics for CO in ZIF-8 is very interesting. Often, (though not always) in systems for which the kinetics of adsorption has been explored, it has been found that the equilibration times are monotonic functions of loading [27,28]. For example, the equilibration times for effectively spherical sorbates on exfoliated graphite or on bundles of closed carbon nanotubes become shorter as the sorbent loading increases [23,24], while linear sorbates such as butane or pentane sorbed on exfoliated graphite have equilibration times that increase with sorbent loading [29]. This is not the case for CO in ZIF-8: the equilibration data for CO in ZIF-8 is clearly non-monotonic, as shown in Fig. 4.

We have studied the kinetics of adsorption in ZIF-8 for two other sorbates: O_2 [20] and Xe [16]. The isotherms of both of these gases have two sub-steps present below saturation (not the three sub-steps that are present for CO) [16,20]. As noted before, synchrotron X-ray diffraction has shown that gate-opening occurs for Xe in ZIF-8 [15]; while inelastic neutron scattering has established that there is no gate-opening for O_2 in ZIF-8 [18]. For both Xe and O_2 in ZIF-8 there are increases in the equilibration times at loadings corresponding to their respective higher-loading sub-steps [16,20]. The increase in the equilibration times measured for both Xe and O_2 in ZIF-8, however, are much smaller than the one measured for CO in ZIF-8 at the highest-loading sub-step. Consequently, we can infer that it is unlikely that the origin of the large increase in equilibration times for CO at the highest-loading sub-step is the same as those for the much smaller increases observed for Xe and O_2 at their respective sub-steps in ZIF-8.

The general trend for the loading dependence of the equilibration times for O_2 and Xe in ZIF-8 (with the exception of the small peak in the higher loading sub-step region) is that the equilibration times decrease as the loading increases [16,20]. Computer simulations of rare gases in flexible ZIF-8 have found that the self-diffusion increases as the loading increases (it was observed in the simulations that the presence of a sorbate atom in a cage makes it easier for an atom to diffuse into a neighboring cage) [30]. This result may provide an explanation for the observed global trends (except for the small peak region) in the equilibration times for a number of gases in ZIF-8.

Besides CO, N_2 in ZIF-8 is the other system known to exhibit three sub-steps below saturation [13,18]. It was suggested that the observed increase in the time needed to reach equilibrium could be the result of the presence of non-zero electric multipoles in these two sorbates (dipole for CO and quadrupole for N_2). [13].

A computer simulation study for N_2 in ZIF-8 explored the self-diffusion of N_2 as a function of sorbent loading [31]. This computational study reports that at high loadings, starting at gate-opening, there is no enhancement of the self-diffusivity. This result is somewhat counter-intuitive, because an increase in self-diffusivity would be expected to accompany an increase in the size of the windows. As the loading increases further, the simulations find a drop of two to three orders of magnitude in the self-diffusivity [31]. The simulations find that there is rearrangement of the N_2 molecules associated with the structural transition, and that at high loadings, closer packing of the N_2 molecules results in stronger interactions between the sorbate and sites on the linkers [31]. In turn, this leads to the decrease in the self-diffusivity [31]. It is likely that the increases that we observe in the equilibration times are at least partly due to similar effects.

In addition to electrostatic interactions between the CO and the ZIF-8 framework, there are other factors that may influence the equilibration times for this system; they include the size and the shape the sorbate molecule.

The effect of molecular size on the equilibration times could, to some extent, be explored by referring to the behavior of Kr sorbed in ZIF-8, since Kr has a very similar size to CO and N_2. Unfortunately, this rare gas has not been studied in ZIF-8 over a range of temperatures that could allow us to carry out a comparison with the results for CO presented here. Clearly it would be useful to conduct adsorption isotherm studies for Kr in ZIF-8 not only because of the comparisons that could be made between the results of such a study and those for N_2 and CO, but also because it would allow to contrast the behavior of Kr with those of Xe, a larger rare gas has been demonstrated to exhibit gate-opening [15] and Ar, a smaller rare gas which has been shown not to exhibit this phenomenon [18].

We can gain some insights into the importance of molecular shape for the de-termination of equilibration times by looking at results available for other systems. A recent study of CO_2 in ZIF-8 reported that there was a general decreasing trend in the equilibration times as the loading of the sorbent increases [21]. Since CO_2 is linear, as are N_2 and CO, it appears unlikely that the linear shape of CO is a determinant factor in its unusual equilibration time behavior.

There is one significant difference between the computer simulation results for the self-diffusion of N_2 in ZIF-8 mentioned above [31] and our experimental results for CO: while the simulations find that the self-diffusion decreases by more than two orders of magnitude as the loading increases beyond the gate-opening region and that this trend is never reversed [31], in our experiments we observe a rapid decrease in the equilibration times as the loading is increased beyond the highest-loading sub-step, and the saturated vapor pressure is approached. This difference in behavior results from the fact that the experimental system has finite ZIF-8 particles, and hence, these particles have an external surface. This is not the case for the simulations. In the experiments, when the sites inside the ZIF-8 particles are filled, adsorption occurs on the ZIF-8 particles' exterior and soon after bulk CO condensation occurs there. The adsorption equilibration times for bulk CO on the surface of the ZIF-8 particles are shorter than the equilibration times inside the pores of the ZIF-8, thus explaining the apparent discrepancy between simulations and experiment.

4.2. Evolution of isotherm features with temperature

The fact that the relative pressures at which the intermediate- and highest-loading isotherm sub-steps for CO in ZIF-8 increase towards the saturated vapor pressure as the temperature increases (see Fig. 5) is consistent with the behavior we have observed for O_2 [20] and Xe [16]

in ZIF-8. For these two sorbates, just as is the case for CO, the straight lines resulting from plotting the logarithm of the pressures at the midpoints of the respective higher sub-steps, as a function of the inverse of the isotherm temperature, intersect the saturated vapor pressure line at sufficiently high temperature. What is observed for those two other systems at temperatures above the intersection of the lines is that the sub-steps are no longer resolvable in the isotherm data [16,20]. Because of experimental limitations we were not able to conduct isotherm measurements up to the temperatures at which the curves corresponding to the intermediate- and highest-loading sub-steps intersect the saturated vapor pressure curve for CO in ZIF-8. However, from fits to the CO data at the midpoints of these sub-steps (see Fig. 5), we expect that the intermediate-loading sub-step for CO will not be observed at temperatures above 134.414 K and that the highest-loading sub-step will be absent from the isotherm above 124.763 K [19] Both of these temperatures are below the critical temperature for CO (which occurs at 134.45 K). [26].

The expectation that the intermediate-loading step for CO should disappear as the temperature increases is consistent with the fact that we observe that the loading interval corresponding to this sub-step decreases significantly in size as the temperature increases. It should be noted that for Xe in ZIF-8 there is convincing evidence from structural [15] and from NMR [32] studies that indicates that gate-opening is still occurring for this system, even in a temperature region that is well above the one at which sub-steps in the isotherms are no longer observed.

4.3. Isosteric heat of adsorption

Fig. 6 displays the dependence of the isosteric heat of adsorption on loading for CO in ZIF-8. Two maxima are present in the isosteric heat of adsorption data: there is a broad peak that reaches a maximum near 12600 μmol/g. That sorbent loading value coincides with the intermediate-loading sub-step in the isotherms. The second, much sharper, peak in the isosteric heat for CO occurs at a loading of about 16500 μmol/g, which agrees very well with the region where the highest-loading sub-step is present in the isotherm data. The other two systems for which the dependence of the isosteric heat on loading has been examined in detail, O_2 and Xe, have only one peak present in the isosteric heat, and it occurs at values of the loading that corresponds to the single highest-loading isotherm sub-steps that are present for them. [16,20].

As was noted in the Introduction, disagreements regarding the nature of the isotherm sub-steps remain [10,12,13,15,17,18]. The inelastic neutron scattering study conducted for CO was not carried out as a function of loading; so, while it demonstrates that once the loading of ZIF-8 with CO is complete there is gate-opening in the system, it does not identify whether gate-opening occurred at the highest or at the intermediate sub-step in the isotherm below saturation. While we cannot identify the nature of the sub-steps in this study, by combining the presence of a very sharp peak in the isosteric heat of adsorption with the very large increase in the equilibration times occurring at the same range of loadings, corresponding to the highest loading sub-step below saturation in the isotherm for CO, we can provide reasonable speculation regarding its nature. It is possible that the behavior of the isosteric heat and that of the equilibration times in the region of the highest sub-step below saturation is the result of molecular reorientation of the CO resulting from electrostatic interactions between the CO dipoles and between the CO dipoles and electrical charges in the framework. There would be heat released as a result of the molecular reorientation (which should result is a more ordered system); and, it is likely that the time frame for the reorientation of the sorbed molecules would be slow at the high sorbent loadings at which this phenomenon is occurring. Structural measurements performed as a function of sorbent loading for CO in ZIF-8 (analogous to those conducted for Xe in ZIF-8) [15] should be able to clarify this issue.

5. Conclusion

Adsorption isotherms measured for CO in ZIF-8 for temperatures between 72.67 and 104.56 K confirm the existence of three sub-steps before saturation for CO in ZIF-8. [13,18].

The equilibration times behave non-monotonically with increasing loading; there are maxima in this quantity at loadings that correspond to the intermediate-loading sub-step, and, to the highest-loading sub-step. The maximum in the equilibration time at highest-loading isotherm step is larger than the one for the intermediate-loading step by more than an order of magnitude (it is approximately larger by a factor of thirty).

Our results for the equilibration times in the loading sub-step regions for CO were compared to those for O_2 [20] and Xe [16] in ZIF-8 and with recent computer simulations for N_2 [31] in ZIF-8. While both O_2 and Xe in ZIF-8 exhibit maxima in the equilibration times corresponding to the regions where their respective isotherms exhibit sub-steps, these maxima are more than an order of magnitude smaller than those measured for the highest-loading sub-step for CO in ZIF-8. This suggests that the large increase for CO has a different origin from those for the other two sorbates.

The isosteric heat of adsorption dependence on sorbent loading for CO in ZIF-8 exhibits two peaks: one broad, with a maximum at a loading corresponding to the intermediate sub-step in the sorption isotherms; and a sharp peak at a loading corresponding to the gate-opening sub-step for this system.

The correspondence between the sorbent loadings at which the isotherm sub-steps are present, and those at which maxima are present in both the equilibration times, and, in the isosteric heat of adsorption strongly suggests that these two features are connected. Combining these results we speculate that a possible explanation for the highest-loading isotherm sub-step is a reorganization of the sorbed molecules as a result of electrostatic interactions between the dipoles and with electrical charges in the framework.

We also suggest two experiments that would be helpful for further exploring the nature of the sub-steps present in the adsorption of some gases in ZIF-8.

Acknowledgements

One of us (ADM) gratefully acknowledges very illuminating conversations with Prof. Joaquin Silvestre-Albero regarding linker-flipping in ZIF-8.

References

[1] P. Silva, S.M. Vilela, J.P. Tome, F.A.A. Paz, Multifunctional metal– organic frameworks: from academia to industrial applications, Chem. Soc. Rev. 44 (19) (2015) 6774–6803.
[2] K. Vellingiri, J.E. Szulejko, P. Kumar, E.E. Kwon, K.-H. Kim, A. Deep, D.W. Boukhvalov, R.J. Brown, Metal organic frameworks as sorption media for volatile and semi-volatile organic compounds at ambient conditions, Sci. Rep. 6 (2016) 27813.
[3] E. Barea, C. Montoro, J.A. Navarro, Toxic gas removal–metal–organic frameworks for the capture and degradation of toxic gases and vapours, Chem. Soc. Rev. 43 (16) (2014) 5419–5430.
[4] Y. He, W. Zhou, G. Qian, B. Chen, Methane storage in metal–organic frameworks, Chem. Soc. Rev. 43 (16) (2014) 5657–5678.
[5] R.B. Getman, Y.-S. Bae, C.E. Wilmer, R.Q. Snurr, Review and analysis of molecular simulations of methane, hydrogen, and acetylene storage in metal–organic frameworks, Chem. Rev. 112 (2) (2011) 703–723.
[6] S. Kitagawa, R. Kitaura, S.-i. Noro, Functional porous coordination poly- mers, Angew. Chem. Int. Ed. 43 (18) (2004) 2334–2375.
[7] M. O'Keeffe, O.M. Yaghi, Deconstructing the crystal structures of metal– organic frameworks and related materials into their underlying nets, Chem. Rev. 112 (2) (2011) 675–702.
[8] M. Eddaoudi, D.F. Sava, J.F. Eubank, K. Adil, V. Guillerm, Zeolite-like metal–organic frameworks (ZMOFs): design, synthesis, and properties, Chem. Soc. Rev. 44 (1) (2015) 228–249.
[9] X.-C. Huang, Y.-Y. Lin, J.-P. Zhang, X.-M. Chen, Ligand-directed strategy for zeolite-type metal–organic frameworks: Zinc (ii) imidazolates with unusual zeolitic

topologies, Angew. Chem. 118 (10) (2006) 1587–1589.
[10] K.S. Park, Z. Ni, A.P. Cote, J.Y. Choi, R. Huang, F.J. Uribe-Romo, H.K. Chae, M. OKeeffe, O.M. Yaghi, Exceptional chemical and thermal stability of zeolitic imidazolate frameworks, Proc. Natl. Acad. Sci. 103 (27) (2006) 10186–10191.
[11] H. Hayashi, A.P. Cote, H. Furukawa, M. O'Keeffe, O.M. Yaghi, Zeolite A imidazolate frameworks, Nat. Mater. 6 (7) (2007) 501.
[12] D. Fairen-Jimenez, S. Moggach, M. Wharmby, P. Wright, S. Parsons, T. Duren, Opening the gate: framework flexibility in ZIF-8 explored by experiments and simulations, J. Am. Chem. Soc. 133 (23) (2011) 8900–8902.
[13] C.O. Ania, E. Garcıa-Perez, M. Haro, J. Gutierrez-Sevillano, T. Valdes- Solıs, J. Parra, S. Calero, Understanding gas-induced structural deformation of ZIF-8, J. Phys. Chem. Lett. 3 (9) (2012) 1159–1164.
[14] S.A. Moggach, T.D. Bennett, A.K. Cheetham, The effect of pressure on zif-8: increasing pore size with pressure and the formation of a high- pressure phase at 1.47 GPa, Angew. Chem. 121 (38) (2009) 7221–7223.
[15] O. Magdysyuk, F. Adams, H.-P. Liermann, I. Spanopoulos, P. Trikalitis, M. Hirscher, R. Morris, M. Duncan, L. McCormick, R. Dinnebier, Understanding the adsorption mechanism of noble gases Kr and Xe in CPO-27-Ni, CPO-27-Mg, and ZIF-8, Phys. Chem. Chem. Phys. 16 (43) (2014) 23908–23914.
[16] D.H. Gallaba, A.G. Albesa, A.D. Migone, Evidence of gate-opening on Xenon adsorption on ZIF-8: an adsorption and computer simulation study, J. Phys. Chem. C 120 (30) (2016) 16649–16657.
[17] M.E. Casco, Y. Cheng, L. Daemen, D. Fairen-Jimenez, E.V. Ramos- Fernandez, A.J. Ramırez-Cuesta, J. Silvestre-Albero, Gate-opening effect in ZIF-8: the first experimental proof using inelastic neutron scattering, Chem. Commun. 52 (18) (2016) 3639–3642.
[18] M.E. Casco, J. Fernandez-Catala, Y. Cheng, L. Daemen, A.J. Ramirez-Cuesta, C. Cuadrado-Collados, J. Silvestre-Albero, E.V. Ramos- Fernandez, Understanding ZIF-8 performance upon gas adsorption by means of inelastic neutron scattering, ChemistrySelect 2 (9) (2017) 2750–2753.
[19] NIST, National Institute of Standards and Technology Tables for Carbon Monoxide Saturated Vapor Pressure, (2017) http://webbook.nist.gov/cgi/cbook.cgi?ID=C124389&Mask=4& Type=ANTOINE&Plot=on#ref-1.
[20] B. Russell, J. Villaroel, K. Sapag, A.D. Migone, O_2 adsorption on ZIF- 8: temperature dependence of the gate-opening transition, J. Phys. Chem. C 118 (49) (2014) 28603–28608.
[21] B.A. Russell, A.D. Migone, Low temperature adsorption study of CO_2 in ZIF-8, Microporous Mesoporous Mater. 246 (2017) 178–185.
[22] I. Yasumoto, Thermal transpiration effects for gases at pressures above 0.1 Torr, J. Phys. Chem. 84 (6) (1980) 589–593.
[23] D. Rawat, V. Krungleviciute, L. Heroux, M. Bulut, M. Calbi, A.D. Migone, Dependence of single-walled carbon nanotube adsorption kinetics on tem- perature and binding energy, Langmuir 24 (23) (2008) 13465–13469.
[24] B.A. Russell, P. Khanal, M.M. Calbi, M. Yudasaka, S. Iijima, A.D. Migone, Sorption kinetics on open carbon nanohorn aggregates: the effect of molecular diameter, Molecules 21 (4) (2016) 521.
[25] J. Rouquerol, F. Rouquerol, P. Llewellyn, G. Maurin, K.S. Sing, Adsorption by Powders and Porous Solids: Principles, Methodology and Applications, Academic Press, 2013.
[26] N.C.W. Stephenson, Malanowski, Enthalpy of Vaporization, (1987) http://webbook.nist.gov/cgi/cbook.cgi?ID=C630080&Mask=4# ref-5.
[27] A.J. Fletcher, K.M. Thomas, Adsorption and desorption kinetics of n- octane and n-nonane vapors on activated carbon, Langmuir 15 (20) (1999) 6908–6914.
[28] A.J. Fletcher, K.M. Thomas, Compensation effect for the kinetics of adsorption/desorption of gases/vapors on microporous carbon materials, Langmuir 16 (15) (2000) 6253–6266.
[29] D.S. Rawat, A.D. Migone, Non-monotonic kinetics of alkane adsorption on single-walled carbon nanotubes, J. Phys. Chem. C 116 (1) (2011) 975–979.
[30] M.V. Parkes, H. Demir, S.L. Teich-McGoldrick, D.S. Sholl, J.A. Greathouse, M.D. Allendorf, Molecular dynamics simulation of framework flexibility effects on noble gas diffusion in HKust-1 and ZIF-8, Microporous Mesoporous Mater. 194 (2014) 190–199.
[31] T. Chokbunpiam, R. Chanajaree, T. Remsungnen, O. Saengsawang, S. Fritzsche, C. Chmelik, J. Caro, W. Janke, S. Hannongbua, N_2 in ZIF- 8: sorbate induced structural changes and self-diffusion, Microporous Mesoporous Mater. 187 (2014) 1–6.
[32] M.-A. Springuel-Huet, A. Nossov, F. Guenneau, A. Gedeon, Flexibility of ZIF-8 materials studied using ^{129}Xe NMR, Chem. Commun. 49 (67) (2013) 7403–7405.